

Magnetic phase stability of monolayers: Fe on $\text{Ta}_x\text{W}_{1-x}$ (001) random alloy as a case study

M. Ondráček*

Institute of Physics ASCR, Cukrovarnická 10, CZ-162 00 Praha 6, Czech Republic

O. Bengone

IPCMS, BP43, 23, rue du Loess, F-67034 Strasbourg Cedex 2, France

J. Kudrnovský, V. Drchal, and F. Máca

Institute of Physics ASCR, Na Slovance 2, CZ-182 21 Praha 8, Czech Republic

I. Turek

Institute of Physics of Materials ASCR, Žitkova 22, CZ-616 62 Brno, Czech Republic

(Dated: February 4, 2022)

We present a new approach to study the magnetic phase stability of magnetic overlayers on nonmagnetic substrates. The exchange integrals among magnetic atoms in the overlayer are estimated in the framework of the adiabatic approximation and used to construct the effective classical two-dimensional Heisenberg Hamiltonian. Its stability is then studied with respect to a large number of collinear and non-collinear magnetic arrangements which include, as special cases, not only ferromagnetic and various antiferromagnetic configurations, but also possible incommensurate spin-spiral structures. This allows us to investigate a broader class of systems than a conventional total energy search based on few, subjectively chosen configurations. As a case study we consider the Fe-monolayer on the random nonmagnetic $\text{bcc-Ta}_x\text{W}_{1-x}$ (001) surface which was studied recently by a conventional approach. We have found a crossover of the ground state of the Fe monolayer from the ferromagnet on the Ta surface to the $c(2 \times 2)$ antiferromagnet on the W surface and that at the composition with about 20 % of Ta an incommensurate magnetic configuration might exist.

PACS numbers: 71.15.Mb, 75.30.Et, 75.70.Ak

I. INTRODUCTION

A deeper understanding of the magnetic ground state as well as of finite-temperature properties of a system with local magnetic moments can be obtained in terms of corresponding exchange interactions. This is particularly true for new, artificially prepared systems, like, e.g., monolayers of magnetic atoms on nonmagnetic substrates. A strong hybridization of the electronic states of the magnetic atoms and of the substrate may significantly influence the magnetic ground state of these systems. We mention as a typical example the Fe-monolayer on $\text{bcc-W}(001)$ substrate. While bcc-Fe in bulk state is a ferromagnet (FM), the Fe-monolayer on the $\text{bcc-W}(001)$ surprisingly has a $c(2 \times 2)$ antiferromagnetic (AFM) ground state, as was recently found by spin-polarized STM measurements¹.

In a subsequent theoretical study, Ferriani *et al.*² demonstrated a strong dependence of the magnetic state of an Fe-monolayer on the substrate by studying its stability on the (001)-face of $\text{bcc-Ta}_x\text{W}_{1-x}$ random substrates. It was found that the ground state of the Fe-monolayer on $\text{Ta}(001)$ is the FM rather than the AFM one and there thus exists an interesting crossover between these two magnetic configurations at an intermediate substrate composition. Results of this study also confirm the robustness of such behavior - even the unrelaxed system exhibits the same behavior although large inward relaxation of about 18 % exists between the Fe monolayer and the first substrate W-layer, which can modify the result quantitatively. The authors of Ref. 2 also clearly demonstrated the usefulness of exchange interactions for a deeper understanding of the phenomenon.

Based on these facts we wish to present here a more general approach to the study of the magnetic stability of such systems. Let us first remind the reader of the approach adopted in paper² as well as in a number of other studies.³⁻⁷ Exchange interactions are estimated by evaluating the total energies of the FM and a few AFM configurations by conventional bandstructure methods. In particular, in the case of Fe overlayer on the $\text{W}(001)$ or $\text{Ta}(001)$, the authors of Ref. 2 chose $c(2 \times 2)$ - and $p(2 \times 1)$ -AFM configurations and mapped the total energy differences of these configurations and of the reference FM state onto the classical two-dimensional Heisenberg Hamiltonian (HH). In this way they obtained two nearest-neighbor exchange couplings. This approach has certain limitations: (i) the choice of AFM configurations is dictated by requirements of simplicity, although any other configuration can be used as well. One has to be aware that if some atypical configuration is chosen, the results can be biased; (ii) the number of determined exchange interactions depends on the number of chosen configurations, which is limited. This is in a striking contrast with the existence of long-range interactions in such systems. For example, the presence of the surface state, e.g., on

the fcc(111) surfaces of noble metals leads to the decay of corresponding exchange interactions with the distance d as d^{-2} (see Ref. 8,9) as compared to the d^{-3} -decay known from bulk systems (the RKKY-interactions). In addition, the bandstructure methods do not yield directly individual exchange interactions, but rather their certain infinite sums; (iii) the use of conventional bandstructure methods is strongly complicated in the presence of disorder, either in the magnetic overlayer or in the substrate. On the other hand, if the substrate disorder is weak, a simple approach (the virtual-crystal approximation) can be successfully used as it was done in Ref. 2 for the case of Fe-overlayer on the TaW-alloy substrate.

An alternative approach is to estimate magnetic interactions among magnetic atoms directly by evaluating the energy cost related to small rotations of spins at arbitrarily chosen two sites with the help of the adiabatic theorem and the Green function method. This approach, first introduced by Lichtenstein *et al.*¹⁰ for bulk ferromagnets and by Oguchi *et al.*¹¹ for bulk paramagnets within the disordered local moment (DLM) state, was then successfully generalized to a number of magnetic systems including magnetic overlayers on crystal substrates¹² (for further magnetic systems see the review paper¹³). In this method the limitations mentioned above are removed. As the method is formulated in the real space, the systems without perfect translational symmetry (e.g. random alloys, overlayers, and surfaces) can be treated on an equal footing with the crystals.

One remark concerns the choice of the reference state from which the exchange interactions are extracted. Conventionally, this is the FM state^{10,12,14}, but it is possible to employ also the AFM reference state or any other reference state such as the DLM state. In the DLM state the spin-spin correlations are missing while in the FM- or AFM-states the spins are strongly correlated. The DLM state is thus particularly suitable for discussion of the electronic origin of the magnetic phase stability as no specific magnetic order is assumed in this reference state. A traditional approach to the exchange interactions in the DLM-reference state^{11,15,16} rests on the generalized perturbation method (GPM);¹⁷ however, the final formula can also be obtained from the method of infinitesimal rotations of local moments applied to a random binary alloy. This equivalence is briefly sketched in Section II and in the Appendix.

Once the exchange interactions are found, and it should be noted that they can be found even for very distant pairs of spins, one can study the ground state of the classical HH. In this way one can search over much broader class of possible magnetic systems, including incommensurate configurations, than it is possible by using a conventional supercell approach. It should be noted, however, that the supercell approach can be highly accurate and useful and we wish to point out the usefulness and complementarity of both above mentioned approaches for various aspects of the magnetic stability rather than to argue that one approach is better as compared to the other.

II. FORMALISM

The electronic properties of the Fe-overlayer on random $\text{Ta}_x\text{W}_{1-x}$ (001) substrate will be studied in the framework of the tight-binding linear muffin-tin orbital (TB-LMTO) method combined with the coherent potential approximation (CPA) to treat alloy disorder in the substrate as well as the magnetic disorder in the DLM state. The effect of the surface is included in the framework of the surface Green function (SGF) approach¹⁸ which employs a realistic semi-infinite sample geometry (no slabs or periodic supercells). The one-electron potential is treated within the atomic sphere approximation, but the dipole barrier due to the redistribution of electrons in the vicinity of the surface is included in the formalism. The TB-LMTO-SGF method can include the effect of layer relaxations approximately provided that they are known either from high-accuracy ab-initio calculations or from experiment.

An important advantage of the TB-LMTO-SGF approach is the possibility to estimate exchange interactions between magnetic atoms in the overlayer. We will describe such magnetic interactions in terms of the two-dimensional classical Heisenberg Hamiltonian,

$$H = - \sum_{i \neq j} J_{ij} \mathbf{e}_i \cdot \mathbf{e}_j, \quad (1)$$

in which J_{ij} denotes the exchange integral between Fe-spins at sites i and j on the surface, and \mathbf{e}_i and \mathbf{e}_j are unit vectors in the directions of the local magnetization on sites i and j , respectively.

Exchange interactions J_{ij} can be evaluated in the the FM reference state and in the framework of the TB-LMTO-SGF method as

$$J_{ij} = \frac{1}{4\pi} \text{Im} \int_C \text{tr}_L \{ \Delta_i(z) \bar{g}_{ij}^\uparrow(z) \Delta_j(z) \bar{g}_{ji}^\downarrow(z) \} dz, \quad (2)$$

where $\Delta_i(z)$ characterizes the exchange splitting of the Fe-atom at the site i , $\bar{g}_{ij}^\sigma(z)$ is the configurationally averaged Green function describing the motion of an electron between Fe-sites i and j in the magnetic overlayer on a random nonmagnetic substrate which corresponds to the spin σ , $\sigma = (\uparrow, \downarrow)$, and the integration is done over the contour

C in the complex energy plane z which starts below the valence band and ends at the Fermi energy. Symbol tr_L denotes the trace over the atomic orbitals ($L \equiv (l, m)$). The quantity $\Delta_i(z)$ is defined in the TB-LMTO method in terms of the potential functions $P_i^\sigma(z)$ of Fe atoms as $\Delta_i(z) = P_i^\uparrow(z) - P_i^\downarrow(z)$. The above expression represents a straightforward generalization of the corresponding bulk expression^{10,13} since it is formulated in the real space. We refer the reader to Refs. 18–20 for details of evaluation of the real-space configurationally averaged Green function $\bar{g}_{ij}^\sigma(z)$ for the magnetic overlayer on a random substrate.

In the DLM-reference state, the exchange interactions J_{ij} bear a standard form of effective pair interactions of the GPM. They are given explicitly by

$$J_{ij} = \frac{1}{4\pi} \text{Im} \int_C \text{tr}_L \{ \tau_i(z) \bar{g}_{ij}(z) \tau_j(z) \bar{g}_{ji}(z) \} dz, \quad (3)$$

where the $\bar{g}_{ij}(z)$ is the spin-independent configurationally averaged Green function in the DLM state between Fe-sites i and j . The electronic structure of the DLM state is treated in an alloy analogy, i.e., the Fe-sites are randomly occupied by two Fe-species with equal probability, representing local Fe-moments pointing in two opposite directions. The quantity $\tau_i(z)$ is defined as $\tau_i(z) = t_i^\uparrow(z) - t_i^\downarrow(z)$, where the symbols $t_i^\sigma(z)$ ($\sigma = \uparrow, \downarrow$) refer to single-site t -matrices of the TB-LMTO method describing scattering due to both magnetic species on the i -th site with respect to a spin-independent effective DLM medium, see Eq. (A.6). In the Appendix, the form of Eq. (3) is derived from the previous formula, Eq. (2), applied to the DLM state within the alloy analogy.

The exchange integrals J_{ij} characterize magnetic interactions between two particular atomic sites. It is also convenient to define the exchange parameter J_0 that reflects the molecular field experienced by a single moment in the ferromagnetic layer

$$J_0 = \sum_{i \neq 0} J_{0i}. \quad (4)$$

A negative value of this parameter indicates an instability of the FM state. A more detailed analysis of the magnetic stability employs the lattice Fourier transform of the pair exchange interactions J_{ij} , see Section III C; the parameter J_0 represents a special case of the Fourier transformed interaction, namely, its value for zero reciprocal vector, see Eq. (6).

III. RESULTS AND DISCUSSION

The calculations were done assuming the Vegard's law for the bulk lattice constant a of $\text{bcc-Ta}_x\text{W}_{1-x}$ random alloy ($a_{\text{Ta}} = 3.300 \text{ \AA}$ and $a_{\text{W}} = 3.165 \text{ \AA}$). The electronic structure is calculated selfconsistently for a model of the system which consists of 7 atomic layers representing the alloy substrate, one Fe layer, and 4 layers of empty spheres representing vacuum that are embedded between the semi-infinite substrate and the semi-infinite vacuum. Similarly as in Ref. 2, we assume a constant inward layer relaxation of 18 % between the Fe-overlayer and the $\text{bcc}(001)\text{-Ta}_x\text{W}_{1-x}$ substrate. We have employed the *spdf*-basis and the Vosko-Wilk-Nusair exchange-correlation LSDA potential in all calculations. We used 20 points on the contour in the complex energy plane and 210 k-points in the irreducible wedge of the surface Brillouin zone in selfconsistent calculations and up to 19600 k-points in the surface Brillouin zone to calculate exchange integrals for 172 inequivalent neighbors.

A. Density of states

We compare in Fig. 1 the Fe-projected densities of states (PDOS) for an unsupported monoatomic Fe(001) layer (assuming the in-plane lattice constant of bcc-W , but the results for that of bcc-Ta are very similar) with the PDOS for Fe/W(001) and Fe/Ta(001). Results for the FM and for the DLM states are shown. We observe a much stronger effect of hybridization among the Fe-located and the substrate states in the case of the W substrate than for the Ta substrate. The PDOS for Fe on the Ta substrate, especially that for the majority spin, is only weakly broadened as compared to the unsupported Fe layer in striking contrast to the case of the W substrate. We thus argue that the strong Fe-W hybridization is the reason for the AFM ordering on the W-substrate: the ground state of the weakly hybridized Fe/Ta(001) is similar to that of the unsupported Fe layer, namely the FM state. Roughly speaking, the stronger Fe-substrate hybridization also reduces the DOS at the Fermi energy in the non-magnetic state and thus reduces the tendency to ferromagnetism (the Stoner criterion). It should be noted that the generally broader minority PDOS as compared to the majority one is due to the large exchange splitting of Fe electron levels: majority levels

are closer to the nucleus and thus are more strongly bound giving a narrower band and just the opposite holds for the more loosely bound minority bands.

Another indication of a stronger hybridization of the Fe-W states as compared to the Fe-Ta states is documented by Fig. 2, where the concentration dependence of local magnetic Fe-moments evaluated in the FM and DLM states is shown. Generally, a stronger hybridization of Fe-W states results in an increasing difference between FM and DLM magnetic moments. The local magnetic Fe moments for the unsupported Fe layer are large and almost the same (about $3.35 \mu_B$) in both the FM and DLM configurations. A stronger hybridization reduces more the local magnetic moments for the Fe/W(001) overlayer as compared to the Fe/Ta(001) one.

In Fig. 3 we present layer-resolved PDOS for first few top layers of the Fe/W(001) and Fe/Ta(001) systems (averaged over spins) and corresponding bulk substrates. We first note a large similarity between the bulk Ta and W total DOS which justifies the virtual crystal approximation used in Ref. 2 to study the effect of alloy disorder in the substrate. The main difference is the position of the Fermi energy which is shifted downwards in the bcc-Ta because of a smaller number of valence electrons. As a consequence, the Fermi energy lies inside the bonding peak of the bcc-DOS while it is shifted to the energy region between the bonding and antibonding states in the bcc-W. We also mention that only the interface substrate layer and to some extent also the second substrate layer differ noticeably from the bulk substrate while the DOSs of other substrate layers are already quite similar to those of bulk. This is, of course, a typical feature of metallic systems in which the corresponding Friedel-like oscillations (which originate from the presence of an abrupt change of the charge density at the surface) are quickly damped inside the substrate due to the high density of screening electrons.

B. Exchange integrals

Concentration dependence of the exchange integrals J_s for the first few shells of neighboring atoms $s = 1 - 5$ is shown in Fig. 4. First, this figure illustrates the principal difference between the approach used in Ref. 2 and the present approach. In the former method, the total energy differences between three magnetic configurations, namely the FM, $c(2 \times 2)$ - and $p(2 \times 1)$ -AFM configurations, are used to estimate two exchange integrals. One can call this approach the first-principle fitting as compared to the direct first-principle calculation of exchange integrals in our present approach. Clearly, realistic exchange integrals are not limited to the first two shells and, in particular, not in the two-dimensional case where exchange integrals can decay in general more slowly than in the three dimensional case (see e.g. Ref. 8,9). It should be noted that we have plotted the exchange integrals without corresponding degeneracies (multiplicities of equivalent surface atoms in the shells) that are 4 or 8 in the present case.

The most remarkable feature observed in Fig. 4 is a dramatic change of the leading first nearest-neighbor (NN) interaction from the strongly AFM coupling in Fe/W(001) to the FM coupling in Fe/Ta(001). The crossover between the AFM and FM couplings roughly coincides with the crossover between the FM and AFM ground state of the Fe overlayer. The concentration dependence of other interactions on the substrate alloy composition is generally weak. The second NN interaction has the AFM character in the whole concentration range while the third NN interaction is FM-like for a W-rich substrate. The first two NN interactions agree reasonably well with those fitted from total energies for three magnetic configurations² both qualitatively and quantitatively (note that the definitions of the Heisenberg Hamiltonian used in the present paper and in Ref. 2 differ by a factor of two). The quantitative agreement of these NN interactions also proves that the chemical disorder in the TaW alloy substrate, which Ref. 2 treated in a simple virtual crystal approximation but which the present study treats in the CPA, is really weak.

In Fig. 5 we compare the difference between total energies of the DLM and FM phases with the calculated exchange parameter J_0 , Eq. (4), for the DLM reference state adopted in this paper. Overall good agreement between both dependences over the whole concentration range should be pointed out. This confirms that the DLM state is a reasonable reference state for the estimate of exchange integrals. The small deviations are due to approximations inherent to the Heisenberg model (fixed size of local moments, the neglected contribution of induced moments in the substrate).

The observed concentration trend of the first NN interaction and of the relative stability of the FM and DLM states can be understood qualitatively on the basis of general properties of a broad class of physical quantities in tight-binding models as functions of band filling.^{21,22} These quantities include, e.g., total-energy differences, local and non-local susceptibilities, magnetic and chemical interactions, etc.; all of them change their sign due to variation of the Fermi energy across the d -band. In the present case, the position of the Fermi level with respect to the Fe d -band is directly controlled by the concentration of the Ta-W alloy substrate.

Finally, in Fig. 6 we illustrate the convergence of the exchange parameter J_0 , Eq. (4), as a function of the number of shells included in the summation. Note that now the shell degeneracies, N_s , are included. Obviously, the inclusion of about 20 NN shells is sufficient for practical purposes (the deviation of the partial sum from the converged value is less than 1 %). At least 10 shells have to be considered in order to predict the formation of an incommensurate

magnetic ground state of Fe/Ta_{0.2}W_{0.8}(001) (see the next subsection for details). This is demonstrated in the inset of Fig. 6, where the lattice Fourier transform $J(\mathbf{q})$ of the real-space exchange interactions J_{0i} is magnified for the relevant wavevectors \mathbf{q} in the surface Brillouin zone. The position of the minimum of the spin-spiral energy, i.e., the wavevector \mathbf{q} for which $J(\mathbf{q})$ has maximum, begins to approach the converged position for more than 10 shells while about 70 shells are needed to reach the converged position with the precision of 0.1 % of the wavevector \mathbf{q} . The first two dominating NN interactions are obviously not enough to reproduce this local spin-spiral energy minimum.

C. Magnetic stability

Let us consider a class of possible arrangements (the so-called \mathbf{q} -waves) of magnetic moments defined as

$$\mathbf{e}_i = (\sin \theta_i \cos \phi_i, \sin \theta_i \sin \phi_i, \cos \theta_i), \quad (5)$$

where the polar angle $\theta_i = \theta_0$ is a constant and the azimuthal angle $\phi_i = \mathbf{q} \cdot \mathbf{R}_i$ is a function of the position vector \mathbf{R}_i of site i . The energy per lattice site corresponding to the HH (1) $E(\mathbf{q}, \theta_0) = -J(\mathbf{q}) \sin^2 \theta_0 - J(\mathbf{0}) \cos^2 \theta_0$ is expressed in terms of the lattice Fourier transform of the site-dependent exchange integrals

$$J(\mathbf{q}) = \sum_j J_{0j} e^{i\mathbf{q} \cdot \mathbf{R}_{0j}}. \quad (6)$$

It is easy to show that

$$\min_{\mathbf{q}, \theta_0} E(\mathbf{q}, \theta_0) = -\max_{\mathbf{q}} J(\mathbf{q}) \quad (7)$$

and that $\theta_0 = \pi/2$ if the minimum of energy is achieved for $\mathbf{q} \neq \mathbf{0}$. Let us note that $J(\mathbf{q})$ is closely connected to the energies of magnetic excitations (magnons) in the system described by the HH, Eq. (1). The maximum of $J(\mathbf{q})$, or, equivalently, the minimum of $-J(\mathbf{q})$, reached for a particular value of the vector $\mathbf{q} = \mathbf{q}_0$ in the surface Brillouin zone indicates a tendency of the magnetic system to form a magnetic ground state characterized by that wave vector \mathbf{q}_0 . The wave vector $\mathbf{q}_0 = \mathbf{0}$ (point $\bar{\Gamma}$ in the surface Brillouin zone) corresponds to the FM ground state while a nonzero wave vector \mathbf{q}_0 corresponds to a more complex ground state including possible AFM or spin-spiral states. For example, \mathbf{q}_0 at the point \bar{M} of the surface Brillouin zone corresponds to the $c(2 \times 2)$ (checkerboard-like) AFM ground state and \mathbf{q}_0 at the point \bar{X} corresponds to the $p(2 \times 1)$ (row-wise) AFM ground state. A minimum of $-J(\mathbf{q})$ outside any point of high-symmetry in the surface Brillouin zone suggests a tendency to form an incommensurate (spin-spiral) magnetic ground-state structure.

In this way, we are able to investigate the stability of a much broader class of magnetic systems as compared to the conventional total energy search. It should be noted, however, that possible more general ground states are not included in the present search and a more advanced search based on the overlayer Heisenberg Hamiltonian, Eq. (1), would be needed. Finally, we mention that in the present study we neglect the anisotropic part of the effective magnetic Hamiltonian, i.e., the anisotropy that concerns orientation of the spins with respect to the underlying lattice. Thus the relativistic effects (the magnetic anisotropy and the Dzyaloshinskii-Moriya interactions (DMI)) as well as the magnetostatic (magnetic dipole-dipole) interactions are missing in the present analysis. The dipole-dipole pair interactions between the first and second NN Fe-Fe pairs are at least two orders of magnitude weaker (below 0.01 meV) than the typical exchange interactions in the present case. However, their long range contributes significantly to formation of domain walls and it might influence other details of the magnetic order too. It is also known that the DMI can lead to long-range chiral structures due to weakening of FM-interactions, as it happens in the Mn/W(110)²³ and Mn/W(001)²⁴ systems. We note that in a consistent theoretical treatment all possible anisotropic terms would have to be included on the same footing.

The curves of $-J(\mathbf{q})$ plotted in Fig. 7 and especially the positions of their minima reflect the dependence of the magnetic ground state on the composition of the substrate. A clearly pronounced minimum for Fe/W(001) at the \bar{M} point in the surface Brillouin zone confirms the total energy search, namely that the checkerboard $c(2 \times 2)$ -AFM is the ground state of the system. With increasing Ta content, the stability of the $c(2 \times 2)$ -AFM state weakens and for about 20 % of Ta atoms a weak minimum corresponding to an incommensurate state (with the wavevector on the line $\bar{X} - \bar{M}$ close to \bar{M}) develops. It should be noted that this minimum is sensitive to the number of shells included in the evaluation of $-J(\mathbf{q})$ and is missing if we consider only few leading exchange interactions (see previous subsection). We cannot exclude the possibility, however, that this shallow local minimum will disappear when the relativistic effects are included. The magnetocrystalline anisotropy, for example, strengthens the tendency towards collinear AFM alignment and competes with the DMI interaction which promotes the rotating, non-collinear magnetism as it was demonstrated recently for the Fe-double chains on the fcc-Ir(001) surface²⁵. If the Ta content further increases, the $p(2 \times 1)$ -AFM

configuration becomes the ground state as it is illustrated for the case with 50 % of Ta atoms where the minimum of $-J(\mathbf{q})$ occurs at \bar{X} , see Fig. 7. In the Ta-rich alloy the stability of the FM phase increases as compared to the $c(2 \times 2)$ one until for Fe/Ta(001) the wave vector at $\bar{\Gamma}$ (or the FM state) becomes the magnetic ground state.

The observed tendency to a non-collinear ground state for $x \approx 0.2$ can be explained by frustration effects on the square Fe lattice accompanying the dominating first and second nearest-neighbor interactions that are both negative for concentrations $x \leq 0.45$, see Fig. 4. For W-rich substrates ($x \rightarrow 0$), the first nearest-neighbor interaction dominates ($|J_1| \gg |J_2|$) and the $c(2 \times 2)$ AFM ground state is not frustrated. For equiatomic concentrations ($x \rightarrow 0.5$), the second nearest-neighbor interaction is the strongest one ($|J_2| \gg |J_1|$) and the $p(2 \times 1)$ AFM ground state is not frustrated either. However, for compositions around $x \approx 0.25$, both interactions are of comparable magnitudes ($J_1 \approx J_2$) which leads to pronounced frustration of these simple AFM states. Moreover, these AFM states become nearly degenerate at $x = 0.2$, where the two leading interactions satisfy roughly a relation $J_1 = 2J_2$.² The formation of a single- \mathbf{q} spin spiral for $x \approx 0.2$ (or of a more complex spin arrangement not considered here) represents thus a natural consequence of existing interactions in the Fe-monolayer.

Finally, the present results (e.g., the critical concentration for the AFM to FM crossover) can be influenced quantitatively by possible structural changes in real system. A recent study²⁶ indicates a possibility for the B2-ordering in a bulk bcc-TaW alloy over a broad concentration range. Also, a smaller surface energy of bcc-Ta as compared to the bcc-W²⁷ together with the larger size of Ta atoms seems to indicate a possibility for the segregation of Ta-atoms at the bcc-(Ta,W)(001) alloy surface. On the other hand, the qualitative conclusions of the present paper remain unchanged.

IV. CONCLUSIONS

We have developed a new approach to study the magnetic phase stability of magnetic overlayers on non-magnetic substrates. The approach consists in the evaluation of exchange integrals between local magnetic moments in the magnetic overlayer using the adiabatic approximation and the real-space Green function approach. This allows us to use this approach also for magnetic overlayers on a random substrate and/or for random alloy magnetic overlayers. Estimated exchange interactions between pairs of local moments in the overlayer are used to construct the effective two-dimensional Heisenberg Hamiltonian, whose stability with respect to periodic spin excitations is investigated. The maxima of the lattice Fourier transform of the site-dependent exchange integrals are searched for as indications of stable periodic spin structures. Such a search allows one to investigate the stability of a much broader class of possible magnetic configurations as compared to the conventional total energy search which is limited to a few empirically chosen configurations. The present approach can be extended in future to include more general magnetic configurations and/or anisotropic effects (spin-orbit and dipole-dipole interactions); the latter are indispensable for estimation of the corresponding Curie/Neel temperatures. As a case study we have investigated in detail the magnetic phase stability of the Fe overlayer on the bcc-Ta_xW_{1-x}(001) random substrate. The exchange interactions for this system were extracted from the DLM state, which involves no correlation among spins of overlayer atoms. Our results are in good agreement with the results of a recent study based on the total energy search and confirm basic approximations adopted in this study. In addition, we have predicted a possible incommensurate magnetic configuration for the W-rich substrate alloy (at about 20 % of Ta).

Acknowledgments

The research was carried out within the projects AV0Z10100520, AV0Z10100521, and AV0Z20410507 of the Academy of Sciences of the Czech Republic. Financial support was provided by the Grant Agency of the Academy of Sciences of the Czech Republic (Project A100100616) and Czech Science Foundation (Projects 202/07/0456 and 202/09/0775). O. B. would like to acknowledge funding support from the ANR of France, Grant No. ANR-06-NANO-053-01.

Appendix: Method of infinitesimal rotations in the DLM state

The purpose of this Appendix is to show a close relation of the formula (3) for exchange interactions in the DLM-reference state to the well-known formula (2) valid for any collinear reference state, including the FM state. The latter formula for the pair interaction J_{ij} between local moments on lattice sites i and j can be written as

$$J_{ij} = \frac{1}{4\pi} \text{Im} \int_C w_{ij}(z) dz, \quad (\text{A.1})$$

where the integrated function in the TB-LMTO method has a form

$$w_{ij} = \text{tr}_L \left\{ \left(P_i^\uparrow - P_i^\downarrow \right) \bar{g}_{ij}^\uparrow \left(P_j^\uparrow - P_j^\downarrow \right) \bar{g}_{ji}^\downarrow \right\}, \quad (\text{A.2})$$

where the energy argument z of each quantity has been omitted. Here we assume for simplicity that possible chemical disorder (random occupation by different species) is confined to non-magnetic sites whereas the sites i and j in (A.1, A.2) are occupied by a single species with non-zero local moment.

The standard treatment of the DLM state employs the CPA²⁸ which leads to the alloy analogy, i.e., the electronic structure can be obtained from a binary equiconcentration random alloy $A_{0.5}B_{0.5}$ with collinear spin structure, where the spin-dependent potential functions of both components are given by $P_i^{A\sigma} = P_i^{B-\sigma} \equiv P_i^\sigma$ (where $\sigma = \uparrow, \downarrow$, and $-\uparrow = \downarrow$, $-\downarrow = \uparrow$). The symbol A (B) represents atoms with local moments pointing upwards (downwards); for symmetry reasons, the configurationally averaged Green function as well as the coherent potential functions are spin-independent, i.e., $\bar{g}_{ij}^\sigma \equiv \bar{g}_{ij}$ and $\mathcal{P}_i^\sigma \equiv \mathcal{P}_i$.

Exchange interactions in the DLM-reference state can naturally be obtained from energy changes accompanying infinitesimal rotations of local moments that were originally pointing in the same direction. This corresponds to occupation of both sites i and j by the same atomic species, e.g., by A atoms. The configuration average of the exchange interaction J_{ij} leads to its original form (A.1) with the function $w_{ij}(z)$ replaced by

$$w_{ij} = \text{tr}_L \left\{ \left(P_i^{A\uparrow} - P_i^{A\downarrow} \right) \bar{g}_{ij}^{A,A\uparrow} \left(P_j^{A\uparrow} - P_j^{A\downarrow} \right) \bar{g}_{ji}^{A,A\downarrow} \right\}, \quad (\text{A.3})$$

where $\bar{g}_{ij}^{A,A\sigma}$ denotes the conditionally averaged Green function in spin channel σ between sites i and j occupied by atoms A. Note that the conditionally averaged Green functions depend on the spin index. Their values within the CPA and for $i \neq j$ are given by

$$\bar{g}_{ij}^{A,A\sigma} = \tilde{f}_i^{A\sigma} \bar{g}_{ij} f_j^{A\sigma}, \quad (\text{A.4})$$

where the spin-dependent factors on the r.h.s. can be expressed in terms of the spin-independent on-site Green functions \bar{g}_{ii} and coherent potential functions \mathcal{P}_i as

$$\begin{aligned} f_i^{A\sigma} &= [1 + (P_i^\sigma - \mathcal{P}_i) \bar{g}_{ii}]^{-1} \equiv f_i^\sigma, \\ \tilde{f}_i^{A\sigma} &= [1 + \bar{g}_{ii} (P_i^\sigma - \mathcal{P}_i)]^{-1} \equiv \tilde{f}_i^\sigma. \end{aligned} \quad (\text{A.5})$$

The scattering due to the atomic species A and B with respect to the effective DLM-medium is described by spin-dependent single-site t-matrices $t_i^{A\sigma} = t_i^{B-\sigma} \equiv t_i^\sigma$, where

$$t_i^\sigma = f_i^\sigma (P_i^\sigma - \mathcal{P}_i) = (P_i^\sigma - \mathcal{P}_i) \tilde{f}_i^\sigma. \quad (\text{A.6})$$

Their difference can be related to the difference of the potential functions P_i^σ , namely,

$$\begin{aligned} t_i^\uparrow - t_i^\downarrow &= \left(P_i^\uparrow - \mathcal{P}_i \right) \tilde{f}_i^\uparrow - f_i^\downarrow \left(P_i^\downarrow - \mathcal{P}_i \right) \\ &= f_i^\downarrow \left\{ \left[1 + \left(P_i^\downarrow - \mathcal{P}_i \right) \bar{g}_{ii} \right] \left(P_i^\uparrow - \mathcal{P}_i \right) \right. \\ &\quad \left. - \left(P_i^\downarrow - \mathcal{P}_i \right) \left[1 + \bar{g}_{ii} \left(P_i^\uparrow - \mathcal{P}_i \right) \right] \right\} \tilde{f}_i^\uparrow \\ &= f_i^\downarrow \left(P_i^\uparrow - P_i^\downarrow \right) \tilde{f}_i^\uparrow, \end{aligned} \quad (\text{A.7})$$

and, similarly,

$$t_i^\uparrow - t_i^\downarrow = f_i^\uparrow \left(P_i^\uparrow - P_i^\downarrow \right) \tilde{f}_i^\downarrow. \quad (\text{A.8})$$

Substitution of Eq. (A.4) into Eq. (A.3), cyclic invariance of the trace and identities (A.7, A.8) lead to the final expression of the function $w_{ij}(z)$ in the pair interaction J_{ij} (A.1):

$$w_{ij} = \text{tr}_L \left\{ \left(t_i^\uparrow - t_i^\downarrow \right) \bar{g}_{ij} \left(t_j^\uparrow - t_j^\downarrow \right) \bar{g}_{ji} \right\}. \quad (\text{A.9})$$

This result is equivalent to the formula (3) in the main text.

* Electronic address: ondracek@fzu.cz

- ¹ A. Kubetzka, P. Ferriani, M. Bode, S. Heinze, G. Bihlmayer, K. von Bergmann, O. Pietzsch, S. Blügel, and R. Wiesendanger, Phys. Rev. Lett. **94**, 087204 (2005).
- ² P. Ferriani, I. Turek, S. Heinze, G. Bihlmayer, and S. Blügel, Phys. Rev. Lett. **99**, 187203 (2007).
- ³ P. Kurz, G. Bihlmayer, and S. Blügel, J. Phys.: Condens. Matter **14**, 6353 (2002).
- ⁴ D. Spišák and J. Hafner, Phys. Rev. B **65**, 235405 (2002).
- ⁵ D. Ködderitzsch, W. Hergert, W. M. Temmerman, Z. Szotek, A. Ernst, and H. Winter, Phys. Rev. B **66**, 064434 (2002).
- ⁶ P. Novák and J. Ruzs, Phys. Rev. B **71**, 184433 (2005).
- ⁷ A. B. Shick, F. Máca, M. Ondráček, O. N. Mryasov, and T. Jungwirth, Phys. Rev. B **78**, 054413 (2008).
- ⁸ K. H. Lau and W. Kohn, Surf. Sci. **75**, 69 (1978).
- ⁹ P. Hyldgaard and M. Persson, J. Phys.: Condens. Matter **12**, L13 (2000).
- ¹⁰ A. I. Liechtenstein, M. I. Katsnelson, V. P. Antropov, and V. A. Gubanov, J. Magn. Magn. Mater. **67**, 65 (1987).
- ¹¹ T. Oguchi, K. Terakura, and N. Hamada, J. Phys. F: Met. Phys. **13**, 145 (1983).
- ¹² M. Pajda, J. Kudrnovský, I. Turek, V. Drchal, and P. Bruno, Phys. Rev. Lett. **85**, 5424 (2000).
- ¹³ I. Turek, J. Kudrnovský, V. Drchal, and P. Bruno, Philos. Mag. **86**, 1713 (2006).
- ¹⁴ M. Pajda, J. Kudrnovský, I. Turek, V. Drchal, and P. Bruno, Phys. Rev. B **64**, 174402 (2001).
- ¹⁵ L. Szunyogh and L. Udvardi, Philos. Mag. B **78**, 617 (1998).
- ¹⁶ A. V. Ruban, S. Shallcross, S. I. Simak, and H. L. Skriver, Phys. Rev. B **70**, 125115 (2004).
- ¹⁷ A. Bieber and F. Gautier, J. Magn. Magn. Mater. **99**, 293 (1991).
- ¹⁸ I. Turek, V. Drchal, J. Kudrnovský, M. Šob, and P. Weinberger, *Electronic Structure of Disordered Alloys, Surfaces and Interfaces* (Kluwer, Boston, 1997).
- ¹⁹ J. Kudrnovský, I. Turek, V. Drchal, P. Weinberger, N. E. Christensen, and S. K. Bose, Phys. Rev. B **46**, 4222 (1992).
- ²⁰ J. Kudrnovský, I. Turek, V. Drchal, P. Weinberger, S. K. Bose, and A. Pasturel, Phys. Rev. B **47**, 16525 (1993).
- ²¹ V. Heine, J. H. Samson, and C. M. M. Nex, J. Phys. F: Met. Phys. **11**, 2645 (1981).
- ²² V. Heine and J. H. Samson, J. Phys. F: Met. Phys. **13**, 2155 (1983).
- ²³ M. Bode, M. Heide, K. von Bergmann, P. Ferriani, S. Heinze, G. Bihlmayer, A. Kubetzka, O. Pietzsch, S. Blügel, and R. Wiesendanger, Nature **447**, 190 (2007).
- ²⁴ P. Ferriani, K. von Bergmann, E. Y. Vedmedenko, S. Heinze, M. Bode, M. Heide, G. Bihlmayer, S. Blügel, and R. Wiesendanger, Phys. Rev. Lett. **101**, 027201 (2008).
- ²⁵ R. Mazzarello and E. Tosatti, Phys. Rev. B **79**, 134402 (2009).
- ²⁶ P. E. A. Turchi, V. Drchal, J. Kudrnovský, C. Colinet, L. Kaufman, and Z.-K. Liu, Phys. Rev. B **71**, 094206 (2005).
- ²⁷ H. L. Skriver and N. M. Rosengaard, Phys. Rev. B **46**, 7157 (1992).
- ²⁸ B. L. Gyorffy, A. J. Pindor, J. Staunton, G. M. Stocks, and H. Winter, J. Phys. F: Met. Phys. **15**, 1337 (1985).

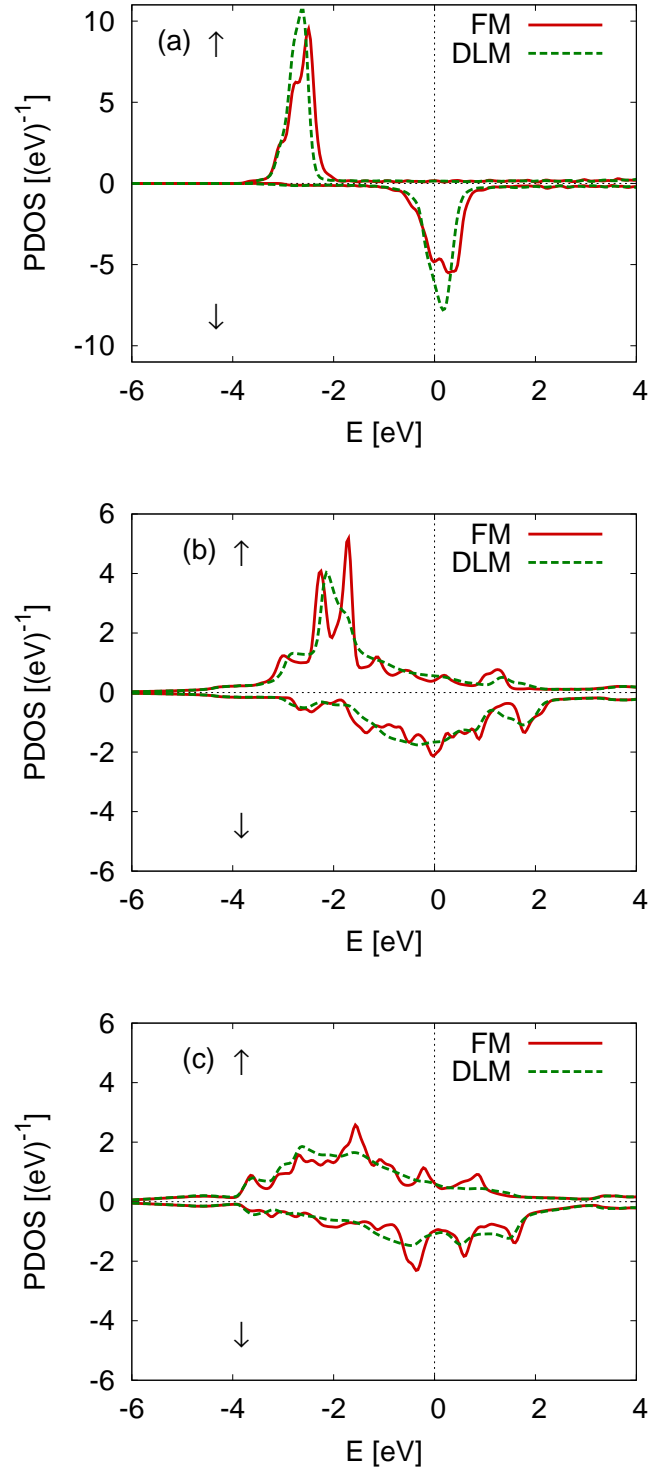


FIG. 1: (color online). Spin-resolved densities of states projected on Fe-atoms for various systems in the ferromagnetic and DLM state: (a) an unsupported Fe monolayer, (b) Fe monolayer on the top of Ta(001) surface, and (c) Fe monolayer on the top of the W(001) surface. The majority (minority) spin states are shown in the upper (lower) panels. The vertical lines denote positions of the Fermi levels.

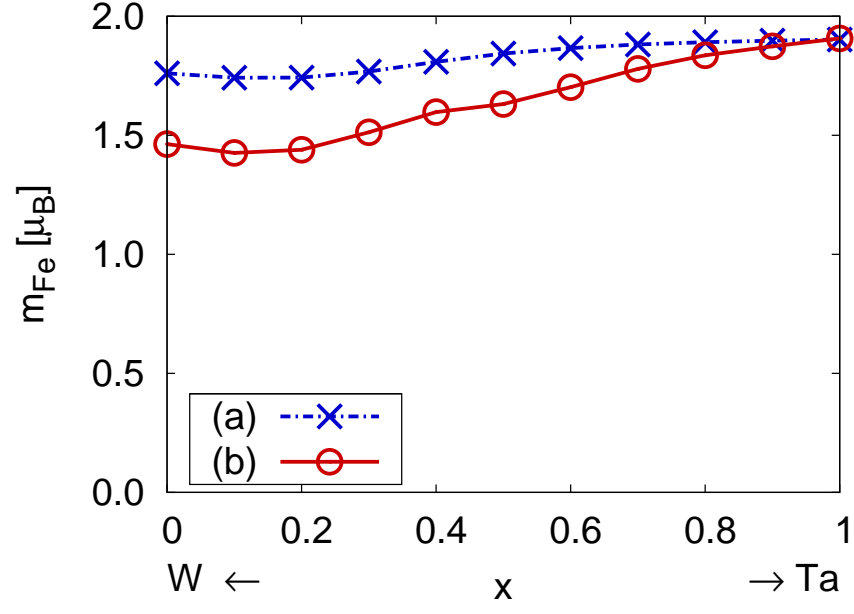


FIG. 2: (color online). The local magnetic moments m_{Fe} of Fe atoms in the monolayer on $\text{Ta}_x\text{W}_{1-x}(001)$ substrate as a function of the alloy composition: (a) the DLM configuration (crosses, $|m_{\text{Fe}}|$ is shown) and (b) the FM configuration (circles).

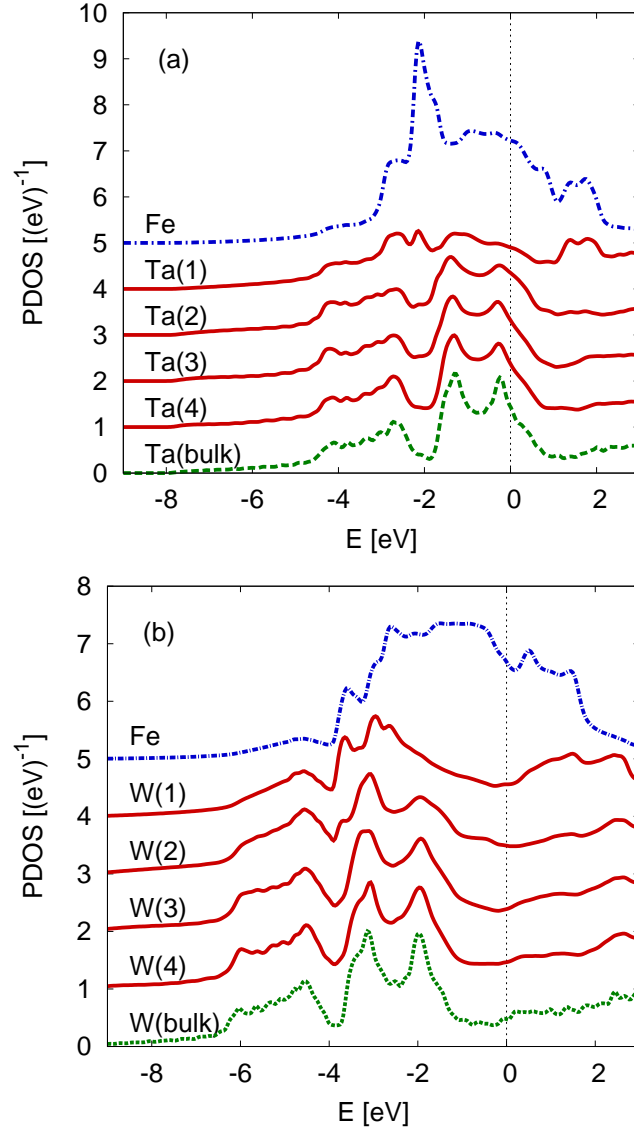


FIG. 3: (color online). Layer-resolved densities of states averaged over spins for the Fe-overlayer in the disordered local moment state (dotted-dashed line), first four substrate layers (full line), and for the bulk substrate (dashed line): (a) Fe/Ta(001) system, and (b) Fe/W(001) system. The curves are shifted vertically with respect to each other. Note the different scale for (a) and (b) plots. The vertical lines denote positions of the bulk Fermi levels.

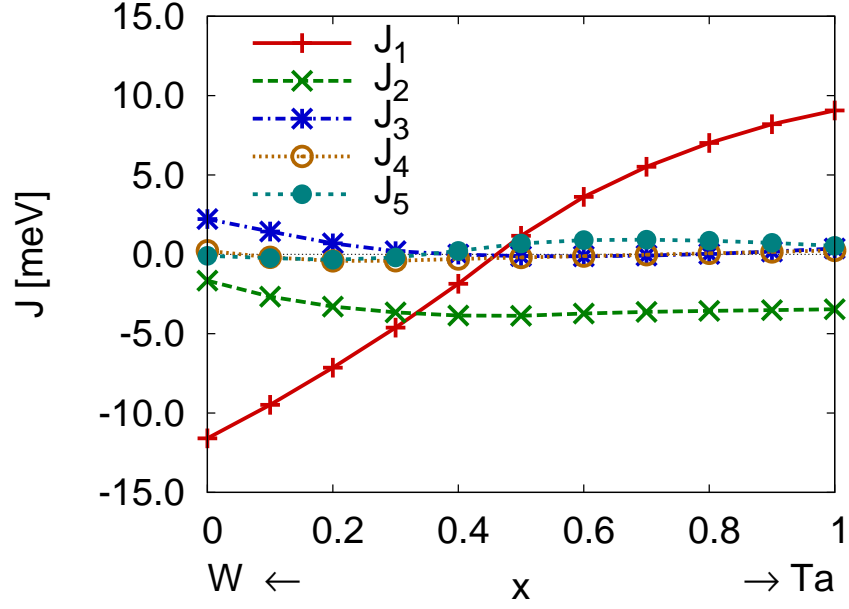


FIG. 4: (color online). Exchange integrals between Fe-atoms (up to the fifth shell) in the Fe overlayer on the $\text{Ta}_x\text{W}_{1-x}$ (001) random alloy surface as a function of the substrate alloy composition.

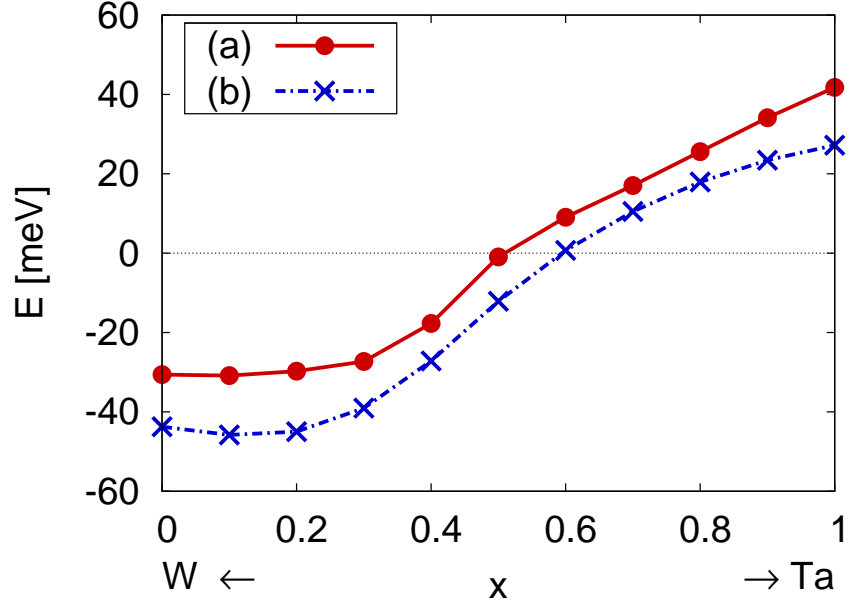


FIG. 5: (color online). (a) The total energy difference of the disordered local moment (DLM) and ferromagnetic (FM) configurations per surface atom ($E_{\text{tot}}^{\text{DLM}} - E_{\text{tot}}^{\text{FM}}$, solid circles). Negative values indicate a tendency to the antiparallel alignment while the positive values indicate a tendency to the parallel alignment of local magnetic moments. (b) Exchange parameter J_0 in the reference DLM configuration defined as the sum of corresponding exchange interactions J_{0i} in the Fe-overlayer (crosses).

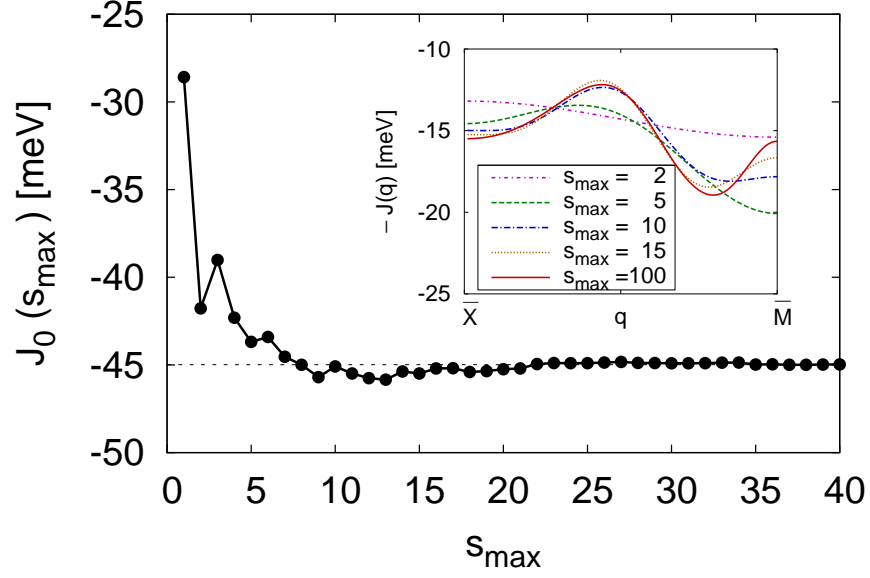


FIG. 6: (color online). The partial sum of the exchange integrals, $J_0(s_{\max}) = \sum_{s=1}^{s_{\max}} N_s J_s$ for the Fe/Ta_{0.2}W_{0.8}(001) system as a function of the shell number s_{\max} . J_s is the exchange integral for the atomic shell s and N_s is the corresponding shell degeneracy, i.e., the number of equivalent atoms in a given shell. The dependence of the lattice Fourier transform $-J(\mathbf{q})$ (see Fig. 7(b)) on the number of shells s_{\max} used in the Fourier transform is shown in the inset. The last of the curves in the inset ($s_{\max}=100$) is essentially a converged result with respect to the shell number.

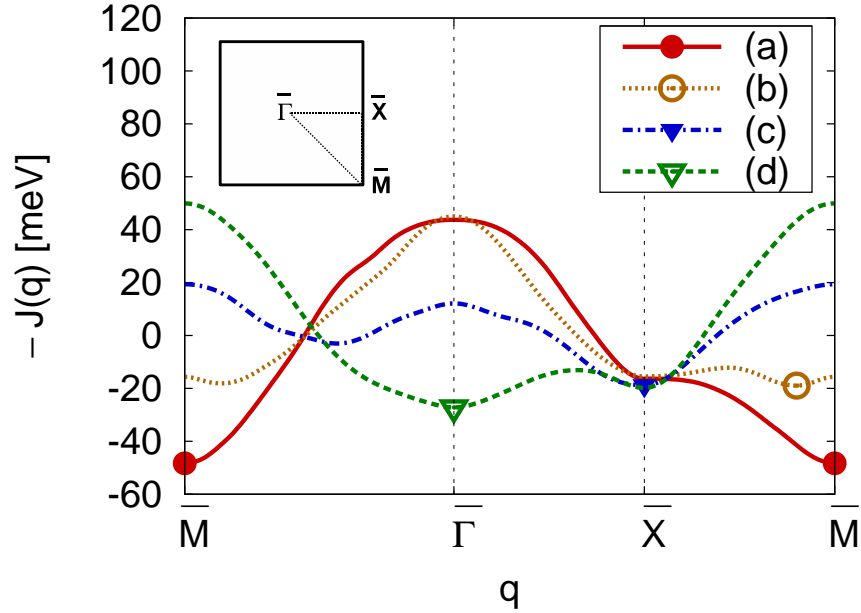


FIG. 7: (color online). The lattice Fourier transform $J(\mathbf{q})$ of exchange integrals in the Fe overlayer as defined by Eq. (6) along a chosen path in the first surface Brillouin zone plotted for different substrate alloy compositions: (a) bcc Fe/W(001), (b) bcc Fe/Ta_{0.2}W_{0.8}(001), (c) bcc Fe/Ta_{0.5}W_{0.5}(001), and (d) bcc Fe/Ta(001). The minimum of $-J(\mathbf{q})$ for each substrate composition is indicated by a symbol on the corresponding curve. The inset shows the first surface Brillouin zone and the corresponding high-symmetry points.